

CHARACTERIZATION OF AIRBORNE PARTICULATE MATTER IN THE METROPOLITAN REGION OF *BELO HORIZONTE*

Fernanda V. F. Tavares¹, José Domingos Ardisson¹, Paulo César H. Rodrigues¹, Walter de Brito¹, Waldemar Augusto A. Macedo¹, Vanusa Maria F. Jacomino¹

¹ Centro de Desenvolvimento da Tecnologia Nuclear.
Av. Presidente Antônio Carlos, 6.627. Campus da UFMG - Pampulha - CEP 31270-901. Caixa Postal 941 -
CEP 30123-970. Belo Horizonte - Minas Gerais - Brasil
ferufv@yahoo.com.br

ABSTRACT

In this work soil samples, iron ore and airborne atmospheric particulate matter (PM) in the Metropolitan Region of *Belo Horizonte* (MRBH), State of Minas Gerais, Brazil, are investigated with the aim of identifying if the sources of the particulate matter are of natural origin, such as, resuspension of particles from soil, or due to anthropogenic origins from mining and processing of iron ore. Samples were characterized by powder X-ray diffraction, X-ray fluorescence and ⁵⁷Fe-Mössbauer spectroscopy. The results showed that soil samples studied are rich in quartz and have low contents of iron mainly iron oxide with low crystallinity. The samples of iron ore and PM have high concentration of iron, predominantly well crystallized hematite. ⁵⁷Fe-Mössbauer spectroscopy confirmed the presence of similar iron oxides in samples of PM and in the samples of iron ore, indicating the anthropogenic origin in the material present in atmosphere of the study area.

1. INTRODUCTION

Air pollution is a severe environmental problem that has become increasingly worse in urban and/or industrial centers. Particulate matter (PM) is an important air pollutant that can cause various damages to public health (respiratory and cardiovascular problems), ecosystems and materials [1, 2]. Part of the Metropolitan Region of *Belo Horizonte* (MRBH) covers the region of the Iron Quadrangle – geological district of major iron production – in the State of *Minas Gerais* (MG), Brazil. The mining and beneficiation of iron ore activities can release large amounts of PM to the atmosphere, so these particles can be both an important pollutant agent and an indicator of air quality in metropolitan area of *Belo Horizonte*.

Studies in this region indicate high levels of iron (Fe) in the elemental composition of atmospheric PM [3]. Inhalation of Fe may contribute to the formation of free radicals and induce oxidative processes in the human body [4] whereas PM particles once reaching the pulmonary alveoli can cause from respiratory problems to other serious lung diseases. The main objective of this study is to investigate the crystallochemical properties of iron based compounds present in atmospheric PM of MRBH, aiming to identify the sources of those pollutant emissions, whether from natural origin, such as the resuspension of soil particles, or from anthropogenic origin, due to mining and processing of iron ore.

2. EXPERIMENTAL

The region of study comprises part of the Iron Quadrangle of *Minas Gerais* that has an important large mining industry and a large population exposed to air pollution, in particular, particulate matter. The location map of the study area, the sampling points of soil, iron ore and particulate matter are shown in Fig. 1. For this work two samples of particulate matter (PM1 and PM2) were collected in the district of *Jardim Canadá* located in the *Nova Lima* municipality at approximately 16 Km linear from the city center of *Belo Horizonte*. *Nova Lima* is an important city of MRBH that concentrates numerous mines activities (Fig.1).

Samples of PM (PM1, PM2) were taken with a brush from the surface of leaves of trees located in specific points of the study area and stored in properly identified polyethylene bottles. Soil samples (S1, S2, S3 and S4) were collected from the ground surface (0-10 cm) at points located in the surrounding areas of those where PM was collected. The samples taken are representative of the different types of soil present in the area of study. Samples of iron ore (M1, M2, M3 and M4) were collected in the vicinity of the collection points of PM. These areas belong to the geological *Cauê* Fomation, the most important mineralized level in the Iron Quadrangle.

Soil samples and iron ore were dried in air, when necessary, and then manually ground in an agate degree until the particle size was smaller than 200 mesh. All samples were characterized by X-ray diffraction (XRD), X-ray fluorescence (XRF) and by ^{57}Fe -Mössbauer spectroscopy (MS), an essential technique for the characterization of soil and atmospheric PM [5-10]. Measurements of XRD were performed at room temperature on an automatic Rigaku diffractometer with $\text{CuK}\alpha$ radiation from $(2\theta) = 4$ to 80° . The X-ray fluorescence analysis, were performed in a Shimadzu EDX-720, with a rhodium tube and silicon-lithium detector. The ^{57}Fe -Mössbauer spectra in transmission geometry were obtained using a conventional spectrometer, with constant acceleration, and a ^{57}Co source on a Rh matrix at room temperature. The measurements were done at room temperature (RT) and at 80K without application of an external magnetic field. For one of the soil samples (sample S1) the measurement was done at 20K. Isomer shift values were quoted relatively to the metallic α -Fe. Resonant curves were least-squares fitted to Lorentzian functions with the software NORMOSTTM-90 (developed by R. A. Brand, at Laboratorium für Angewandte Physik, Universität Duisburg, D-47048, Duisburg-Germany).

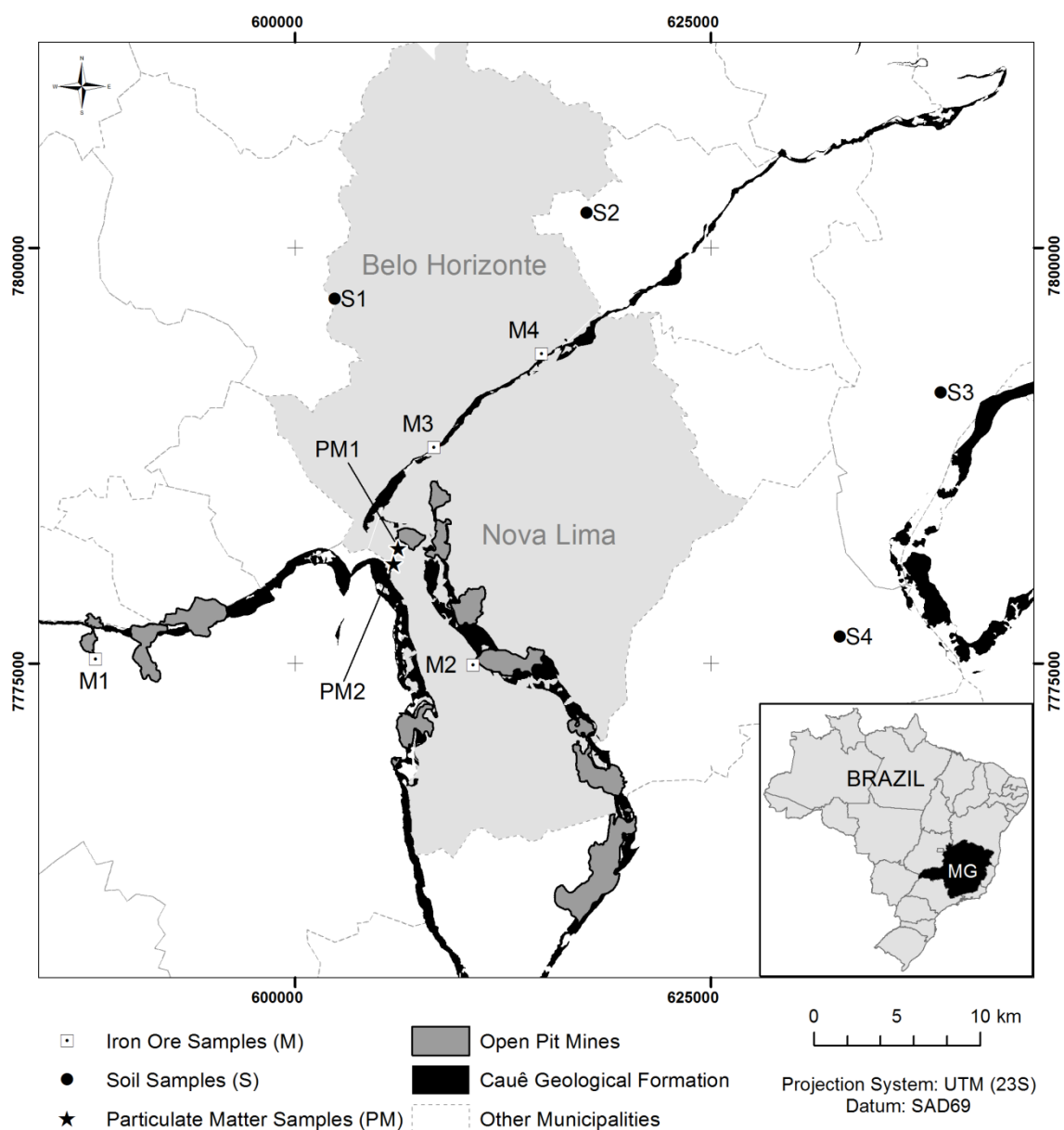


Figure 1: Location map. Sampling of soils (S), iron ore (M) and particulate matter (PM).

3. RESULTS AND DISCUSSION

Typical room temperature (RT) ^{57}Fe -Mössbauer spectra of soil samples, iron ore and PM at are shown in Fig. 2. The spectra of the soil samples, identified by S1, S2, S3 and S4 (Fig. 2a), are formed by the superposition of two contributions, one characterized by a central paramagnetic doublet, approximately symmetrical, and the other one characterized by a ferromagnetic contribution represented by a six line spectrum (sextet). The paramagnetic fraction may be assigned to the presence of Fe-silicates, due to the substitution of Fe^{3+} in tetrahedral sites by Al^{3+} and/or the presence of iron oxides in a superparamagnetic state [8, 9,

11-13]. The magnetic fraction has hyperfine parameters characteristics of hematite ($\alpha\text{-Fe}_2\text{O}_3$) (Table 1) [11-13]. Room temperature ^{57}Fe -Mössbauer spectra of samples of iron ore, M1, M2, M3 and M4 (Fig. 2b) were fitted with a majority sextet characteristic of $\alpha\text{-Fe}_2\text{O}_3$ with relative subspectral area ranging between 70 and 100% and a minority sextet in sample M3 associated to goethite ($\alpha\text{-FeOOH}$) (Table 2). The room temperature ^{57}Fe -Mössbauer spectra of PM (Fig. 2c) are were fitted with two subspectra: a sextet with $\sim 80\%$ relative area identified as hematite and a doublet assigned to superparamagnetic goethite (Table 3).

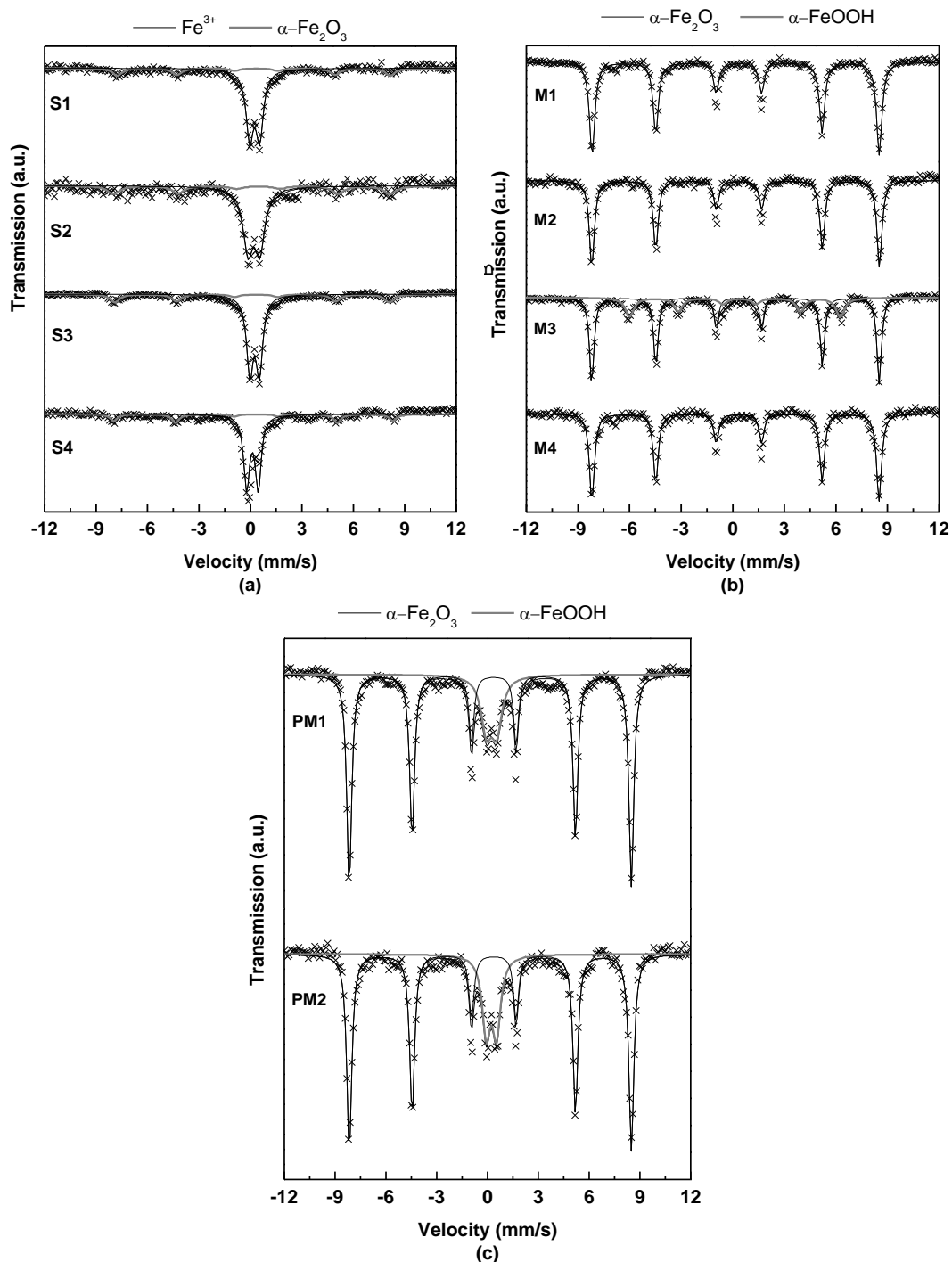


Figure 2: Typical room temperature ^{57}Fe -Mössbauer spectra for samples of (a) Soil (S), (b) Iron Ore (M) and (c) Particulate Matter (PM).

Table 1: ^{57}Fe -Mössbauer parameters of soil samples at RT and 80K. (δ = isomer shift relative to $\alpha\text{-Fe}$; Δ = quadrupole splitting; ε = quadrupole shift; BHF = hyperfine magnetic field; RA = relative spectral areas).

Sample	Temperature	Phase	δ (± 0.05) (mm/s)	ε, Δ (± 0.05) (mm/s)	BHF (± 0.5) (Tesla)	RA (%)
S1	RT	$\alpha\text{-Fe}_2\text{O}_3^{\text{a}}$	0.37	-0.13	49.3	25
		Fe^{3+}	0.36	0.58	-	75
	80 K	$\alpha\text{-FeOOH}^{\text{b}}$	0.53	-0.37	48.3	11
		$\alpha\text{-Fe}_2\text{O}_3$	0.48	-0.18	52.5	39
		$\text{Fe}_5\text{HO}_8\cdot 4\text{H}_2\text{O}^{\text{c}}$	0.55	-0.30	44.2	13
		$\text{FeTiO}_3^{\text{d}}$	0.54	2.38	-	12
		$\gamma\text{-FeOOH}^{\text{e}}$	0.48	0.65	-	25
S2	RT	$\alpha\text{-Fe}_2\text{O}_3$	0.37	-0.38	49.9	27
		Fe^{3+}	0.31	0.68	-	73
	80 K	$\alpha\text{-FeOOH}$	0.36	-0.31	48.7	14
		$\alpha\text{-Fe}_2\text{O}_3$	0.48	-0.25	52.5	24
		$\text{Fe}_5\text{HO}_8\cdot 4\text{H}_2\text{O}$	0.55	-0.24	44.2	11
		FeTiO_3	1.42	2.60	-	10
		$\gamma\text{-FeOOH}$	0.39	0.92	-	41
S3	RT	$\alpha\text{-Fe}_2\text{O}_3$	0.33	-0.24	49.6	26
		Fe^{3+}	0.35	0.55	-	74
	80 K	$\alpha\text{-FeOOH}$	0.49	-0.28	48.3	57
		$\alpha\text{-Fe}_2\text{O}_3$	0.47	-0.14	52.5	10
		$\text{Fe}_5\text{HO}_8\cdot 4\text{H}_2\text{O}$	0.56	-0.30	43.1	9
		FeTiO_3	0.58	2.39	-	9
		$\gamma\text{-FeOOH}$	0.52	0.64	-	15
S4	RT	$\alpha\text{-Fe}_2\text{O}_3$	0.37	-0.18	50.5	24
		Fe^{3+}	0.23	0.68	-	76
	80 K	$\alpha\text{-FeOOH}$	0.48	-0.25	49.3	28
		$\alpha\text{-Fe}_2\text{O}_3$	0.49	-0.15	52.7	10
		$\text{Fe}_5\text{HO}_8\cdot 4\text{H}_2\text{O}$	0.43	-0.28	46.4	27
		FeTiO_3	0.61	2.27	-	5
		$\gamma\text{-FeOOH}$	0.12	0.56	-	30

^aHematite, ^bGoethite, ^cFerrihydrite, ^dIlmenite, ^eLepidocrocite

Table 2: ^{57}Fe -Mössbauer parameters of iron ore samples at RT and 80K.

Sample	Temperature	Phase	δ (± 0.05) (mm/s)	ε, Δ (± 0.05) (mm/s)	BHF (± 0.5) (Tesla)	RA (%)
M1	RT	$\alpha\text{-Fe}_2\text{O}_3^{\text{a}}$	0.37	-0.19	51.8	100
	80 K	$\alpha\text{-Fe}_2\text{O}_3$	0.49	0.35	54.0	100
M2	RT	$\alpha\text{-Fe}_2\text{O}_3$	0.38	-0.20	51.8	100
	80 K	$\alpha\text{-Fe}_2\text{O}_3$	0.49	0.40	54.2	100
M3	RT	$\alpha\text{-Fe}_2\text{O}_3$	0.37	-0.21	51.8	70
		$\alpha\text{-FeOOH}^{\text{b}}$	0.37	-0.26	38.0	30
	80 K	$\alpha\text{-FeOOH}$	0.46	-0.21	50.0	27
M4	RT	$\alpha\text{-Fe}_2\text{O}_3$	0.49	0.42	54.2	73
		$\alpha\text{-Fe}_2\text{O}_3$	0.37	-0.20	51.8	100
	80 K	$\alpha\text{-FeOOH}$	0.43	0.07	51.4	15
		$\alpha\text{-Fe}_2\text{O}_3$	0.49	0.38	54.2	85

^aHematite, ^bGoethite

Table 3: ^{57}Fe -Mössbauer parameters of particulate matter samples at RT and 80 K

Sample	Temperature	Phase	δ ($\pm 0,05$) (mm/s)	ϵ, Δ ($\pm 0,05$) (mm/s)	BHF ($\pm 0,5$) (Tesla)	RA (%)
PM1	RT	$\alpha\text{-FeOOH}^{\text{a}}$	0.35	0.61	-	20
		$\alpha\text{-Fe}_2\text{O}_3^{\text{b}}$	0.38	-0.20	51.7	80
	80 K	$\alpha\text{-FeOOH}$	0.48	-0.08	51.0	29
		$\alpha\text{-Fe}_2\text{O}_3$	0.48	0.35	53.7	71
PM2	RT	$\alpha\text{-FeOOH}$	0.34	0.61	-	23
		$\alpha\text{-Fe}_2\text{O}_3$	0.38	-0.20	51.7	77
	80 K	$\alpha\text{-FeOOH}$	0.43	-0.33	49.7	29
		$\alpha\text{-Fe}_2\text{O}_3$	0.49	0.34	53.7	71

^aGoethite, ^bHematite

^{57}Fe -Mössbauer measurements at 80K were performed in order to better identify the mineralogical phases present in the samples. The spectra of the soil samples (Fig. 3a) were fitted with two doublets and three sextets. The two doublets were assigned to superparamagnetic ilmenite (FeTiO_3) [11-13] and lepidocrocite ($\gamma\text{-FeOOH}$), with very small particles size. Regarding the three sextets, two of them were assigned to hematite ($\alpha\text{-Fe}_2\text{O}_3$) and goethite ($\alpha\text{-FeOOH}$). The quadrupole shift (ϵ) of the former, with values between -0.14 and -0.25 mm/s show that such hematite in the soil has not experienced a Morin transition ($T_M \sim 265\text{K}$), in other words, the particles are presumably small and the structure oxide has cations isomorphically substituted Fe^{3+} , most likely by Al^{3+} [14,15]. The third sextet with hyperfine field of ~ 44 T was assigned to low crystallinity ferrihydrite ($\text{Fe}_5\text{HO}_8 \cdot 4\text{H}_2\text{O}$). This identification is based on studies by Murad [16] in natural samples of mineral soil, which showed superparamagnetic behavior at RT and blocking temperatures ranging from 28 to 115K. According to Carpenter et al. [17] ^{57}Fe -Mössbauer measurements at 20K on poorly crystallized, synthetically prepared ferrihydrite presented a sextet of widened lines with negligible quadrupole splitting and average hyperfine field (BHF) of 45 T. Measurements at 20K in one of the soil samples (sample S1) (Fig. 4) showed that one of the sextets has IS = 0.44 mm/s, $\epsilon = 0.0$ mm/s and BHF = 44.7 T, confirming the presence of ferrihydrite. Although samples S1, S2, S3 and S4 are from different types of soil, the ^{57}Fe -Mössbauer spectra revealed no significant differences among them. The ^{57}Fe -Mössbauer spectra of samples of iron ore at 80K (Fig. 3b) were fitted with two sextets characteristic of hematite, with subspectral area between ~ 70 and 100%, and goethite. ^{57}Fe -Mössbauer spectra of PM at 80K (Fig. 3c) were fitted with two sextets assigned to hematite and goethite with 71% and 29% subspectral area, respectively. Interestingly the hematite at 80K in the iron ore and PM present positive quadrupole shift, suggesting that $T = 80\text{K}$ is below the Morin transition ($T_M \sim 265\text{K}$), which occurs for pure and well-crystallized hematite [14].

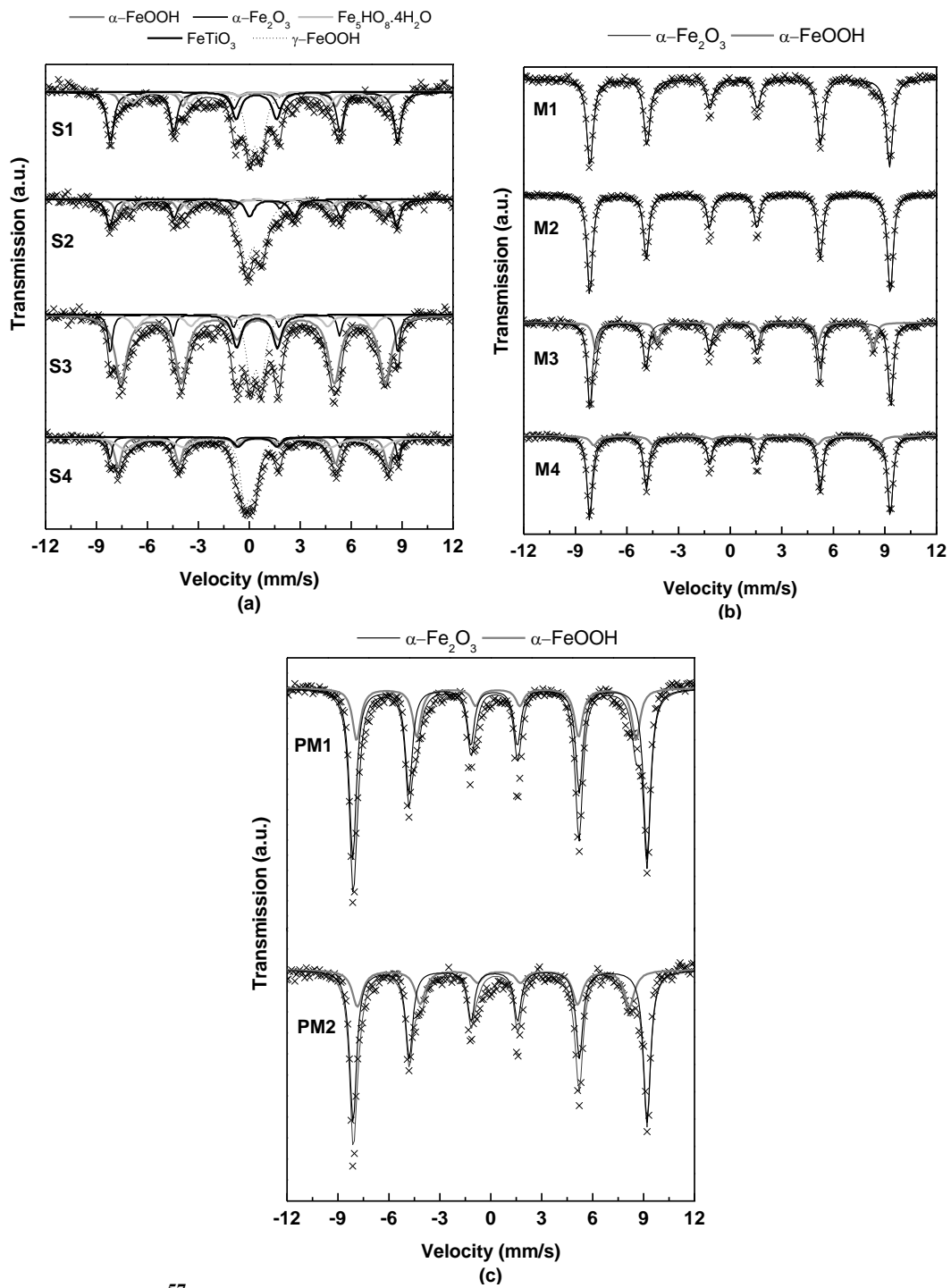


Figure 3: Typical ^{57}Fe -Mossbauer spectra obtained at 80K for samples of (a) Soil (S), (b) Iron Ore (M) and (c) Particulate Matter (PM).

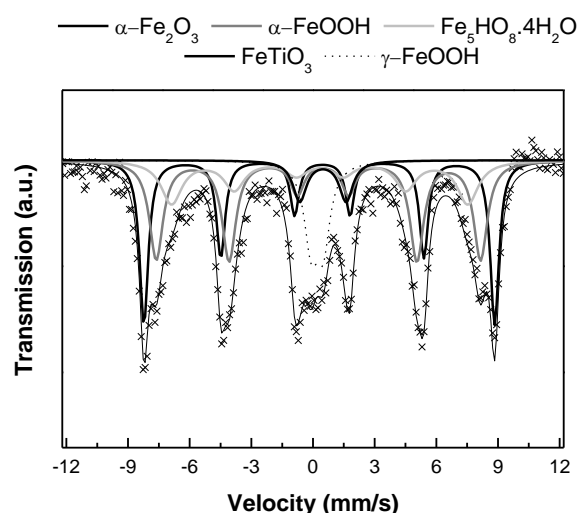


Figure 4: Typical ^{57}Fe -Mossbauer spectra measured at 20K on soil sample.

Comparing the room temperature and 80K results of the ^{57}Fe -Mössbauer spectroscopy for samples of soil, iron ore and PM, it can be seen that the hyperfine parameters of iron compounds in the samples of iron ore and particulate matter are similar: iron ore and PM samples showed high levels of iron, predominantly hematite with a high degree of crystallization. This similarity may be related to the common origin of the PM and iron ore, indicating that the mining and processing of iron ore in the region under study contribute to the highest percentage of PM present in the atmosphere of the district of *Jardim Canadá*, compared to the contribution of resuspension of soils particles.

Moreover, the results of the chemical analysis by XRF (Table 4) on samples S1, S2, S3 and S4 showed that the most abundant elements in the soil composition are silicon (~40 and 70 w%) and aluminum (~13 and 28 w%); iron (~3 and 12 w%) and potassium, calcium, sodium, titanium, magnesium, chromium, manganese, phosphorus and sulfur with low contributions. The content of organic matter, determined gravimetrically after heating the samples at 850 °C for 1 hour, vary between 5 and 35 w%. Samples M1, M2, M3 and M4 XRF revealed high concentration of iron (~70 and 90 w%), silicon (5 and 20 w%), aluminium (1 and 8%) and low concentration of sulfur, calcium, manganese, phosphorus and organic material. The most abundant elements in in the particulate matter samples (PM1 and PM2) were Fe (~40 w%), Al and Si (~13 w%), Ca (~5 w%), while, Ti, K, S, P, Mn, Cr were found in proportions below 1 w%.

Table 4: Chemical composition of samples of soil (S), iron ore (M) and particulate matter (PM) determined with X-ray fluorescence spectroscopy

Sample	Si (%)	Al (%)	Fe (%)	K (%)	Ca (%)	Na (%)	Mg (%)	Ti (%)	Cr (%)	Mn (%)	P (%)	S (%)	O.M. ^a (%)
S1	43.0	28.2	6.1	0.3	0.3	-	-	0.8	-	-	-	0.1	21.2
S2	53.4	25.4	2.8	3.1	0.3	-	0.3	0.3	-	-	-	0.1	14.3
S3	30.7	19.9	12.3	0.7	0.2	-	-	1.1	0.1	0.1	0.1	0.1	34.7
S4	70.2	13.8	5.7	2.1	0.2	2.2	-	0.3	-	0.3	-	0.1	5.1
M1	4.7	7.5	87.4	-	-	-	-	-	-	0.2	-	0.2	-
M2	10.0	0.9	88.6	-	-	-	-	-	-	0.3	-	0.2	-
M3	21.3	1.8	73.3	-	-	-	-	-	-	0.4	-	0.1	3.0
M4	4.6	3.3	90.5	-	0.3	-	-	-	-	0.7	0.4	0.2	-
PM1	12.8	13.0	44.6	0.6	6.5	0.0	0.0	0.8	0.1	0.3	0.3	0.5	20.6
PM2	13.8	13.0	39.9	0.9	4.3	0.0	0.0	0.7	0.1	0.3	0.3	0.6	26.1

^aOrganic Matter

In addition, powder XRD results for the soil samples confirmed the predominance of compounds of Si, Al and low levels of Fe, K and Na, as seen by XRF. Among the compounds identified in the XRD patterns of the soil samples (Fig. 5), quartz was the most abundant (SiO_2), followed by kaolinite ($\text{Al}_2\text{Si}_2\text{O}_5(\text{OH})_4$), gibbsite ($\alpha\text{-Al}_2\text{O}_3 \cdot 3\text{H}_2\text{O}$), muscovite ($\text{KAl}_2(\text{AlSi}_3\text{O}_{10})(\text{OH})_2$), hematite (Fe_2O_3), albite ($\text{NaAlSi}_3\text{O}_8$), microcline (KAlSi_3O_8) and goethite (FeOOH). For samples of iron ore (Fig. 6) it was possible to identify the predominance of hematite (Fe_2O_3), with a high degree of crystallinity and other minerals such as quartz (SiO_2), kaolinite ($\text{Al}_2\text{Si}_2\text{O}_5(\text{OH})_4$), goethite (FeOOH), gibbsite ($\text{Al}_2\text{O}_3 \cdot 3\text{H}_2\text{O} - \alpha$) and microcline (KAlSi_3O_8). The XRD patterns of the PM samples (Fig. 7) revealed the predominance of hematite (Fe_2O_3) and quartz (SiO_2). Minerals such as gibbsite ($\alpha\text{-Al}_2\text{O}_3 \cdot 3\text{H}_2\text{O}$), calcite (CaCO_3), goethite (FeOOH), microcline (KAlSi_3O_8), albite ($\text{NaAlSi}_3\text{O}_8$), kaolinite ($\text{Al}_2\text{Si}_2\text{O}_5(\text{OH})_4$), dolomite ($\text{CaMg}(\text{CO}_3)_2$) and muscovite ($\text{KAl}_2(\text{AlSi}_3\text{O}_{10})(\text{OH})_2$) were identified.

Hence, XRD confirmed the predominance of hematite with a high degree of crystallization in the iron ore and PM samples, as observed by XRF and ^{57}Fe -Mössbauer spectroscopy.

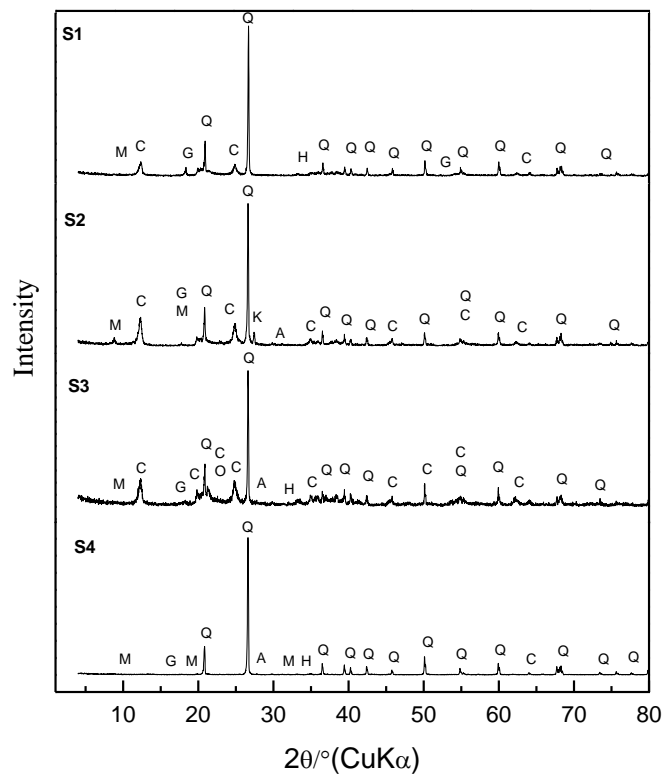


Figure 5: Powder X-ray diffraction patterns of soil samples. C: kaolinite, Q: quartz, G: gibbsite, H: hematite, O: goethite, M: muscovite, K: microcline, A: albite.

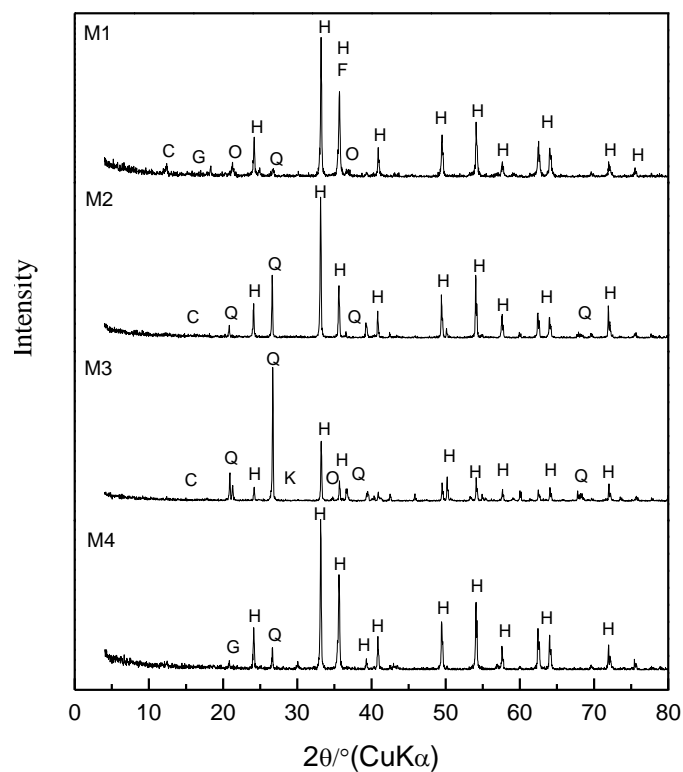


Figure 6: Powder X-ray diffraction patterns of iron ore samples. H: hematite, O: goethite, C: Kaolinite, Q: quartz, G: gibbsite, K: microcline.

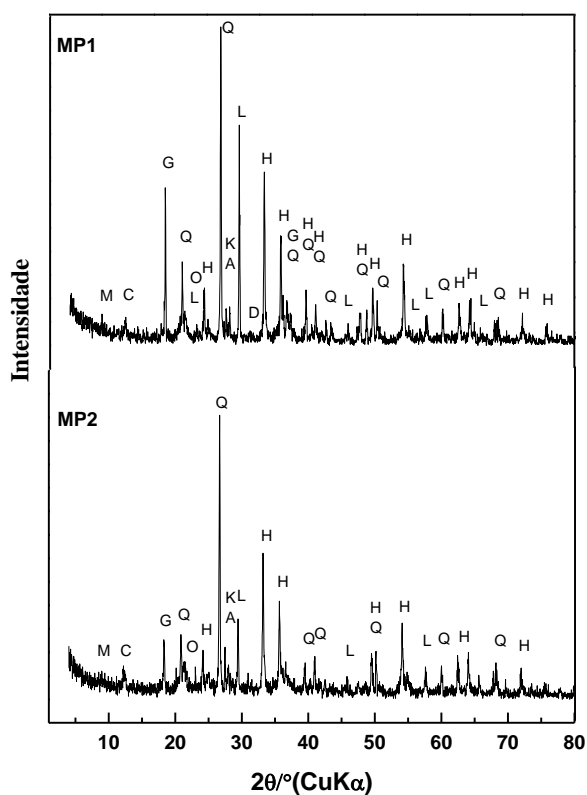


Figure 7: Powder X-ray diffraction patterns of particulate matter. L: calcite, H: hematite, Q: quartz, G: gibbsite, O: goethite, A: albite, C: kaolinite, K: microcline, D: dolomite, M: muscovite.

4. CONCLUSIONS

Soil samples, iron ore and atmospheric particulate matter of MRBH were analyzed by X-ray diffraction, X-ray fluorescence and ^{57}Fe -Mössbauer spectroscopy. Our results show that the soils studied are rich in quartz and have low contents of iron mainly due to poorly crystallized iron oxide. The iron ore and PM samples showed high concentration of iron, predominantly hematite, with a high degree of crystallization. ^{57}Fe -Mössbauer spectroscopy showed that the hematite present in the soil has not experienced a Morin transition ($T_M \sim 265\text{K}$), possibly due to the presence of Al in the structure. On the other hand, the Morin transition ($T_M \sim 265\text{K}$) observed on the hematite present in the iron ore and atmospheric airborne particulate matter (PM) is indicative of hematite of high purity and degree of crystallinity. These differences, only observed by ^{57}Fe -Mössbauer spectroscopy, are essential to evaluate the contribution of the mining and processing of iron ore on the air quality of MRBH. These results confirm the hypothesis that mining and beneficiation of iron ore contribute for the largest percentage of PM in the atmosphere of the study area, *Jardim Canadá* neighborhood. Additional samplings of atmospheric PM are being collected in other neighborhoods in order to validate these results for entire region of study.

ACKNOWLEDGMENTS

We would like to thank Centro de Desenvolvimento da Tecnologia Nuclear (CDTN), Coordenação de Aperfeiçoamento de Pessoal de Nível Superior (CAPES), Conselho Nacional de Desenvolvimento Científico e Tecnológico (CNPq) and Fundação de Amparo à Pesquisa do Estado de Minas Gerais (FAPEMIG).

REFERENCES

1. C. A. Pope III, R. T. Burnett, M. J. Thun, E. E. Calle, D. Krewski, K. Ito, G. D. Thurston, "Lung Cancer, Cardiopulmonary Mortality, and Long-term Exposure to Fine Particulate Air Pollution," *J. Am. Med. Assoc.*, **287**, pp.1132–1141 (2002).
2. K. Donaldson, X. Y. Li, W. MacNee, "Ultrafine (nanometre) particle mediated lung injury," *J. Aerosol Sci.*, **29** (5/6), pp.553–560 (1998).
3. C. O. Viana, M. A. B. C. Menezes, E. C. P. Maia, "Epiphytic lichens on air biomonitoring in Belo Horizonte City, Brazil: a preliminary assessment," *Int. J. Environ. Health*, **5**, pp.324–337 (2011).
4. G. Garçon, P. Shirali, S. Garry, M. Fontaine, F. Zerimech, A. Martin, M. Hanothiaux, "Polycyclic aromatic hydrocarbon coated onto Fe_2O_3 particles: assessment of cellular membrane damage and antioxidant system disruption in human epithelial lung cells (L132) in culture," *Toxicol. Letters*, **117**, pp.25–35 (2000).
5. A. R. Muxworthy, E. Schmidbauer, N. Petersen, "Magnetic properties and Mössbauer spectra of urban atmospheric particulate matter: a case study from Munich, Germany," *Geophys. J. Int.*, **150**, pp.558–570 (2002).
6. B. Kopcewicz, M. Kopcewicz, "Long-term measurements of iron-containing aerosols by Mössbauer spectroscopy in Poland," *Atmospheric Environment*, **35**, pp.3739-3747, (2001).
7. B. Kopcewicz, M. Kopcewicz, "Ecological aspects of Mössbauer study of iron-containing atmospheric aerosols," *Hyperfine Interact.*, **126**, pp.131-135 (2000).

8. B. Kopcewicz, M. Kopcewicz, "Iron-containing atmospheric aerosols," *Hyperfine Interact.*, **111**, pp.179–187 (1998).
9. B. Kopcewicz, M. Kopcewicz, "Mössbauer Study of Iron-Containing Atmospheric Aerosols," *Structural Chemistry*, **2**, pp.303-312 (1991).
10. P. A. Souza Jr., R. S. de Queiroz, T. Morimoto, A. F. Guimarães, V. K. Garg, G. Klingelhöfer, "Precise Indication of Air Pollution Sources," *Hyperfine Interact.*, **139/140**, pp.641–649 (2002).
11. Figueiredo, M. do A. et al., "Óxidos de ferro de solos formados sobre gnaiss do Complexo Bação, Quadrilátero Ferrífero, Minas Gerais," *Pesqui. agropecu. bras.*, **41 (2)**, pp.313–321 (2006).
12. B. A. Ferreira, J. D. Fabris, D. P. Santana, N. Curi, "Óxidos de ferro das frações areia e silte de um nitossolo desenvolvido de basalto," *Rev. bras. cienc. Solo*, **27**, pp.405–413 (2003).
13. N. Curi, P. E. F. Motta, J. D. Fabris, L. C. A. Oliveira, "Espectroscopia Mössbauer na caracterização de compostos ferrosos em solos e sua relação com retenção de fósforo," *Quim. Nova*, **31 (6)**, pp.1467–1471 (2008).
14. Van der Woude, F, "Mössbauer effect in α -Fe₂O₃," *Phys. Stat. Sol.*, **17**, pp.417-432 (1966).
15. E. Murad, U. Schwertmann, "Influence of Al Substitution and Crystal Size on the Room-Temperature Mössbauer Spectrum of Hematite," *Clays and Clay Minerals*, **34 (1)**, pp.1-6 (1986).
16. E. Murad, "The characterization of soils, clays, and Clay firing products," *Hyperfine Interact.*, **111**, pp.251-259 (1998).
17. E. E. Carpenter, J. W. Long, D. R. Rolison, M. S. Logan, K. Pettigrew, R. M. Stroud, "Magnetic and Mössbauer spectroscopy studies of nanocrystalline iron oxide aerogels," *J. Appl. Phys.*, **99**, pp.08N711 (2006).